

A Gap Detector of Linear Synchronous Motors in the Maglev System

Jun Wu, Lu Li, Wenwu ZHou, ZHIqiang Long & Wensen CHang

Mechatronics & Automation School

National University of Defence Technology

Changsha, Hunan, China, 410073

E-mail: junwu@tom.com

ABSTRACT: This paper describes an inductive magnetic sensor for gap detection of linear synchronous motors (LSMs) when high speed maglev trains are moving forward. Because the conductive surface of the primary is tooth and groove profile, the coil geometry is analyzed and optimized to reduce groove effects, namely the output fluctuations of gap signals. The results are presented to indicate that the effective coil is a kind of rectangle flat one whose middle part is sinking. For the sake of avoiding disturbance of the other surrounding magnetic field, EMI method is proposed also.

1 INTRODUCTION

In recent years, high speed maglev train is well developed in China and other countries. To some extent, the train can be regarded as a kind of large linear synchronous motors (LSMs). During propulsion, the gap between the primary and the secondary should be kept constant to avoid thrust ripple. In order to measure gap, a reliable detector is a magnetic type sensor because it can realize non-contact measurement without impair of dust or grease. Figure 1 shows the sensor's theory. When the sensing coil excited by high frequency currents is closing to the conductor, equivalent mutual impedance is changed by eddy currents and static magnetic. The gap distance is reflected as the changes of equivalent output voltage. Calibrating the relation between gap and output, the gap information can be easily measured^{[1],[3]}.

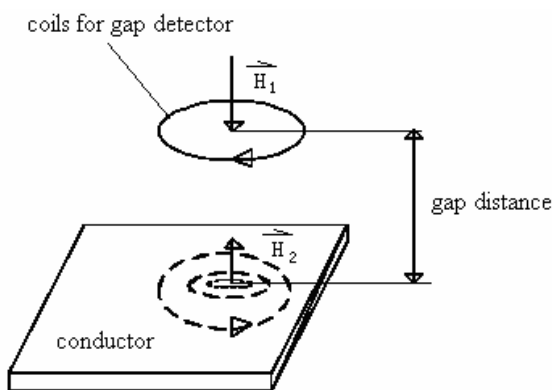


Figure 1: Theory of gap detector

As figure 2 shows, the magnetic sensor is mounted between the magnets. The conductive surface is tooth and groove^{[2],[3],[4]}. If normal inductive sensor is applied, it will induce profile as a fluctuating error into gap signal although it is moving over the stator with the constant distance to the second-

dary. Thus, the first important requirement for the gap detector is that it should be able to sustain the measurement for a conductive surface of tooth and groove profile. Furthermore, there are many fields surround the gap detector, such as moving magnetic field and levitation filed. So it is also important to pay attention to EMC designs for proper work. This paper will discuss the design of the gap detector, especially about how to decrease the fluctuating errors induced by the groove profile. And some EMC method is proposed also.

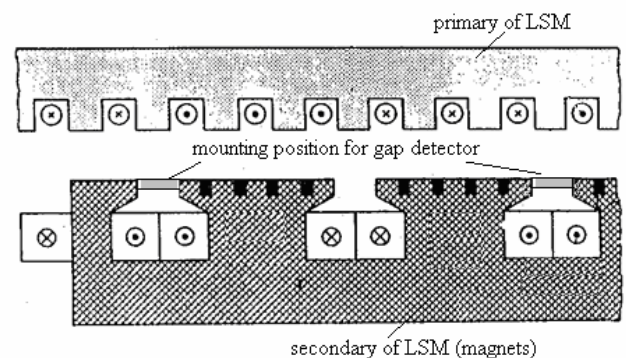


Figure 2: Sketch map of LSM in maglev

2 THE STRUCTURE OF GAP DETECTOR

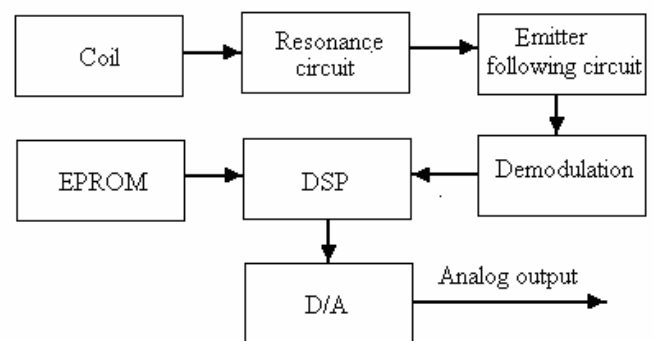


Figure 3: Electrical structure of gap detector

Figure 3 shows the detector's structure which is based on a single chip DSP, ADMC331. The gap information is translated into a high frequency voltage signals by the magnetic couple, as the coil is a part of resonance circuit. Before processed by DSP, signal has to be demodulated. Then, nonlinear compensation, adjustments for temperature compensation and digital filter have been realized by programs. In the end, it is transformed into analogue output. Since ADMC331 has integrated several analogue input channels, programmable timer and digital I/O port, the structure of gap detector can be simplified and performance can be improved as well.

3 COILS DESIGN FOR THE GAP DETECTOR

3.1 Calculation of excitation current

In order to study the behaviour of the detector, an electrical equivalent circuit is generally adopted as Fig. 4. In this circuit, R_0 is the resistor in series with the test coil, C is parallel connection capacitor with coil. R_1 is the resistance of coil. L_1 is inductance of coil. M is mutual inductance between coil and conductor. L_2 is the inductance of conductor. R_2 is the resistor of conductor. ω is the frequency of the excited current. The equivalent reluctance is^[1]

$$Z = \left[R_1 + \frac{R_2 \omega^2 M^2}{R_2^2 + \omega^2 L_2^2} \right] + j\omega \left[L_1 - \frac{\omega^2 M^2 L_2}{R_2^2 + \omega^2 L_2^2} \right] \quad (1)$$

Supposed ω is much higher, that is $\omega L_2 \gg R_2$, yields equation (2),

$$R = R_1 + R_2 \frac{L_1}{L_2} k^2, \quad L = L_1(1 - k^2) \quad (2)$$

$$\text{Where } k = \frac{M}{\sqrt{L_1 L_2}} \circ$$

Thus, yields the excitation current,

$$i_1 = \frac{U_1}{Z} = \frac{U_1}{R_1 + R_2 \frac{L_1}{L_2} k^2 + j\omega L_1(1 - k^2)} \quad (3)$$

And the amplitude of excitation current is,

$$I = \frac{|U_1|}{\sqrt{R_1^2 + R_2^2 \frac{L_1^2}{L_2^2} k^4 - \omega^2 L_1^2 (1 - k^2)^2}} \quad (4)$$

Where $|U_1|$ is the amplitude of excitation voltage.

3.2 Magnetic field analysis of rectangle coil

Since the gap detector is mounted between the magnets, the sensing coil has to be design as a flat rectangle, as it is showed in the figure 5.

Initially, the width of coil is set the same as the width of a groove and a groove. Thus, the coil can always cover a tooth and a groove when gap detec-

tor is moving. As a result, it may induce the same equivalent inductance and there may be fewer fluctuations in the output voltage of gap detector.

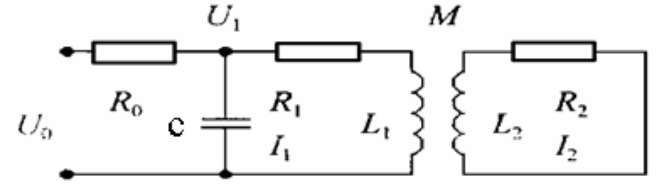


Figure 4: Electrical equivalent circuits for the detector

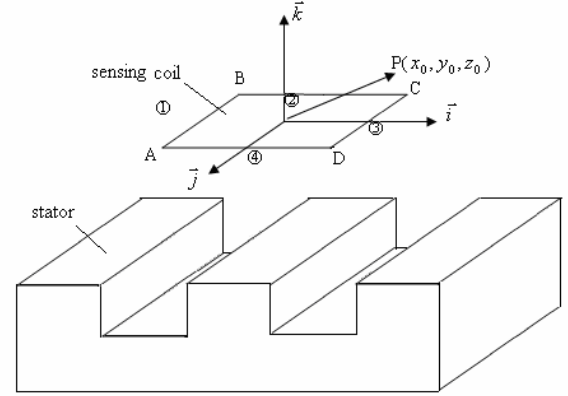


Figure 5: Sensing coil and stator

To verify this idea, magnetic induction of the certain point in the effective sensible area between the gap has been analyzed by Biot-Savart's law. Base the law, the magnetic induction can be calculated as the sum of four section line of the rectangle coil. That is,

$$\vec{B} = \vec{B}_1 + \vec{B}_2 + \vec{B}_3 + \vec{B}_4 \quad (5)$$

Where $\vec{B}_1, \vec{B}_2, \vec{B}_3, \vec{B}_4$ is the magnetic induction induced by AB, BC, CD, DA independently.

Because the stator is a structure of silicon steel lamination, there is less inductive effect by the two section lines, AB and CD. So, the impact is mainly dependent on the other two lines, BC and DA, the magnetic fields are calculated as the following,

$$\vec{B}_2 = \frac{\mu_0 I [(x_0 - a)\vec{k} - z_0\vec{i}]}{4\pi[(x_0 - a)^2 + z_0^2]} (\sin \beta_2 - \sin \alpha_2) \quad (6)$$

Where, $\alpha_2 = \arctg \frac{-(b + y_0)}{\sqrt{(x_0 - a)^2 + z_0^2}}$,

$$\beta_2 = \arctg \frac{b - y_0}{\sqrt{(x_0 - a)^2 + z_0^2}}$$

a, b is half width of line AB, CD and AD, BC respectively.

$$\vec{B}_4 = \frac{\mu_0 I [(x_0 + a)\vec{k} - z_0\vec{i}]}{4\pi[(x_0 + a)^2 + z_0^2]} (\sin \beta_4 - \sin \alpha_4) \quad (7)$$

Where , $\alpha_4 = \arctg \frac{b - y_0}{\sqrt{(x_0 + a)^2 + z_0^2}}$,

$$\beta_4 = \arctg \frac{(b + y_0)}{\sqrt{(x_0 + a)^2 + z_0^2}}$$

I is the amplitude of excitation current.

Magnetic induction distribution is calculated and drawn in the figure 6. Since the inductance is a sum function of whole area of the test coil, the magnetic distribution along \vec{i} axis can be integrated for analysis. That is the result is shown in figure 7.

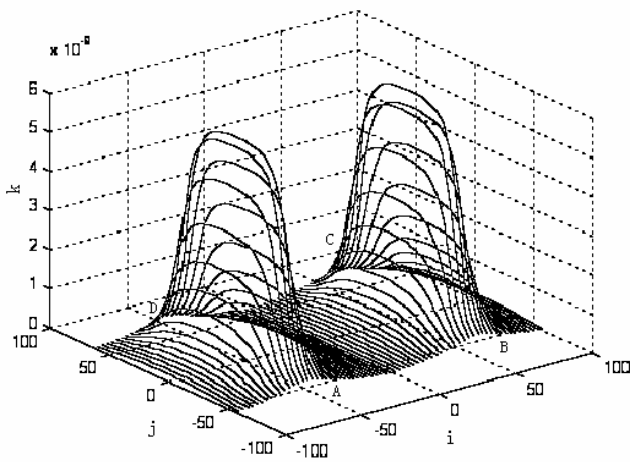


Figure 6: Magnetic induction distribution

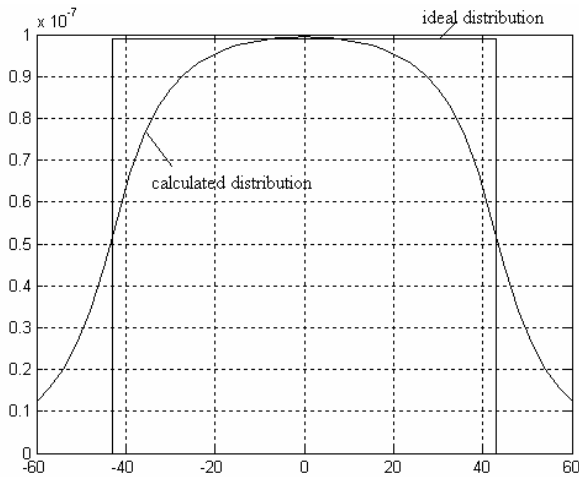


Figure 7: Integrated magnetic induction

In fig.7, the ideal magnetic distribution is a rectangle profile, that is, the magnetic is constant in the coil's cover area and the magnetic is zero out of the area. If it can be realized, the equivalent mutual inductance between conductive primary and test coil will be the same regardless the primary's position to the coil. But the calculated magnetic distribution of rectangle coil is a curve in which the middle part is

quite higher than the two edge side. That may cause much higher fluctuations. Figure 8 has showed this result whose detection error is higher than 1 mm.

3.3 A new designed coil

To approximate the idea rectangle field distribution, the middle part can be sunk to decrease the peak value of field distribution. Thus, it can equal to values at both two edge sides. Based this idea, the middle part of the two lines AD and BC have sunk. Based on this kind of coil, figure 10 and 11 shows that the distribution of magnetic induction in the coil covered area is almost the same, especially at the edge.

Figure 11 has showed this result whose detection error is much more decreased than figure 8. It proves the feasibility of the proposed idea.

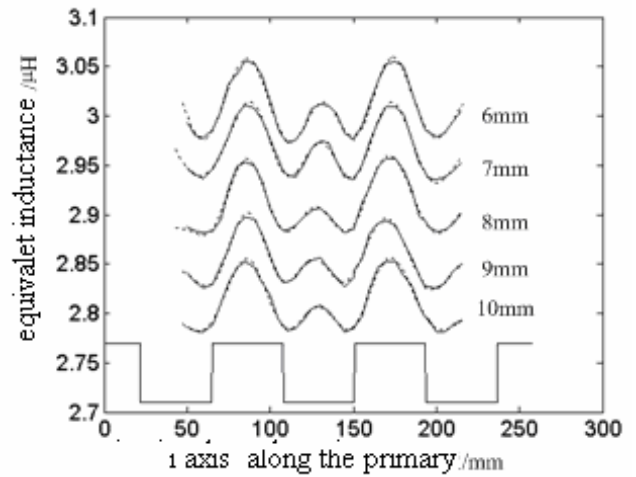


Figure 8: Equivalent inductance of different gap

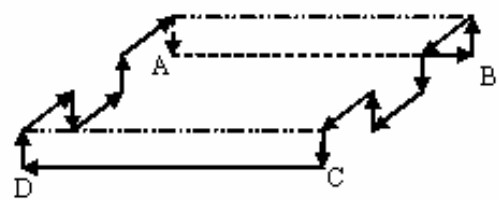


Figure 9: Sketch map of new designed coils

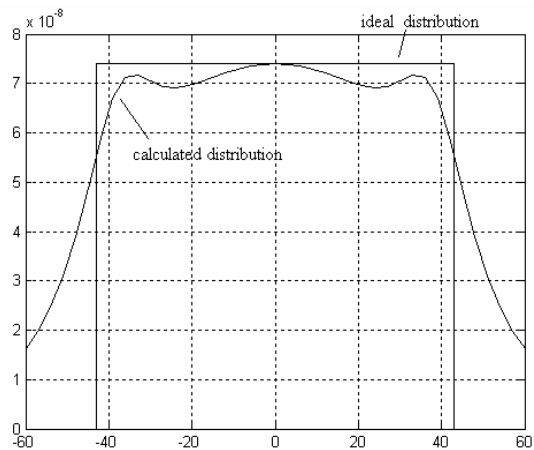


Figure 10: The integrated magnetic induction

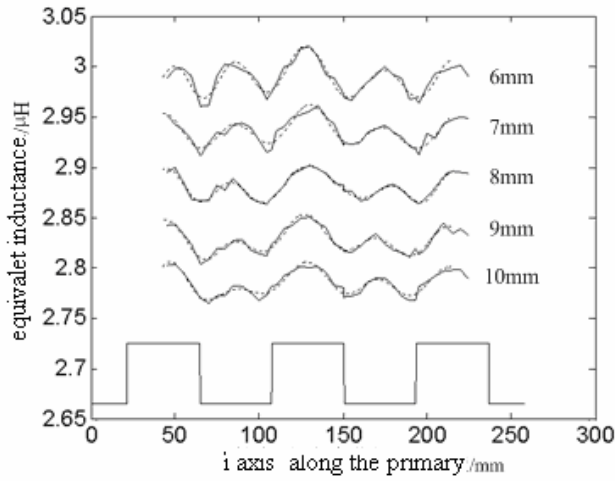


Figure 11: Equivalent inductance of different gap

4 EMC DESIGN FOR THE GAP DETECTOR

Because the gap detector is mounted between the magnets, the field environment is complex. It is important to consider the EMC method. This paper emphasizes on the supply powers. Figure 12 shows that two stage filters have been designed to endure some EMC tests, such as electrical fast transient or burst immunity test and surge immunity test. When input passes through the first filter, the common mode disturbance has been eliminated. And the second filter can eliminated the differential mode disturbance.

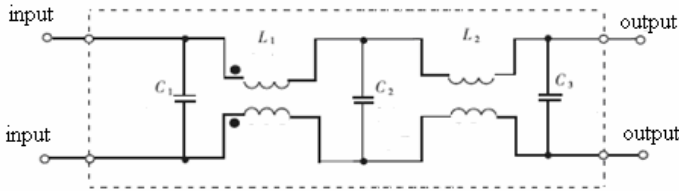


Figure 12: EMI filter circuit

5 TEST RESULTS AND CONCLUSIONS

Based on the above research and analysis, figure 13 shows the measurement results when the gap detector is moving along the primary. It shows that fluctuation error has not higher than ± 0.4 mm when the gap is among the value from 8 mm to 16 mm.

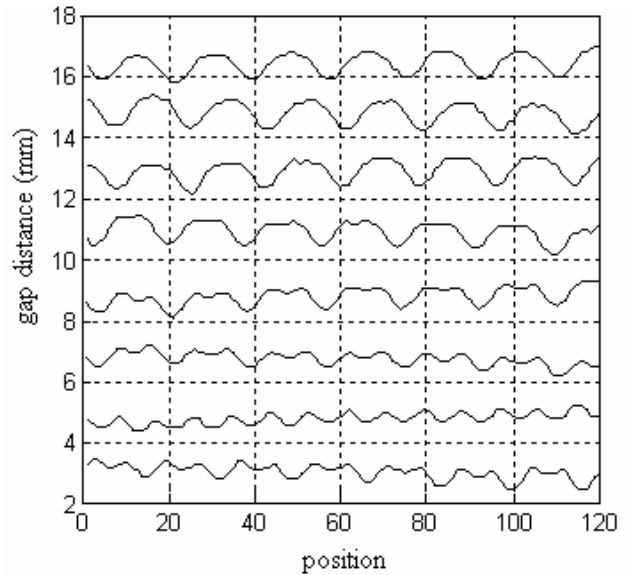


Figure 13. Measurement result of gap detector

Thus, it can be concluded that:

The structure of sinking coil is effective to decrease the fluctuation when the detector is measuring the gap between the coil and primary of LSM. It can eliminate the impact of the tooth and groove profile partly.

The dimension can be optimized for much better result by magnetic analysis.

The EMC method has to be considered for the gap detector because it is surrounded by complex fields. The EMI filter has to be deigned for both common mode and differential mode disturbance.

6 REFERENCES

1. Ren Jilin, Lin Junming, Gao Chunfa. 2000. *Detection by electromagnetic*. Beijing: China Machine Press.
2. Siegfried Ellmann, Ascheim; Joachim Klesing, München; etc. 1998. Method for the reliable determination of the distance of the conductive reaction track from a functional surface of a magnetic levitation vehicle moving relative to the reaction track and a sensor for performing the method . *United States Patent*, Patent number: 5764050
3. Liu Huaqing, Li Zhiye. 1995. *Maglev train in German*. Chengdu: Electronics Science University Press.
4. F. Castelli Dezza, A. Di Gerlando, G.M. Foglia. 2004. Analytical Evaluation of the Electromotive Forces in Synchronous Linear Electrical Machines. *18th International Conference on Magnetically levitated System and Linear Drives*, Shanghai, China, October 25-29.